Separation Science and Technology
Publication details, including instructions for authors and subscription information:
http://www.informaworld.com/smpp/title~content=t713708471

Hydrodynamic Modeling of Droplet Coalescence at Liquid-Liquid Interfaces

Wolfgang Rommel[a]; Walter Meon[b]; Eckhart Blass[a]
[a] CHAIR A FOR CHEMICAL ENGINEERING TECHNICAL, UNIVERSITY OF MUNICH, MUNICH, GERMANY [b] DAGUSSA AG, HANAU/WOLFGANG, GERMANY

To cite this Article Rommel, Wolfgang , Meon, Walter and Blass, Eckhart(1992) 'Hydrodynamic Modeling of Droplet Coalescence at Liquid-Liquid Interfaces', Separation Science and Technology, 27: 2, 129 — 159
To link to this Article: DOI: 10.1080/01496399208018870
URL: http://dx.doi.org/10.1080/01496399208018870

SEPARATION SCIENCE AND TECHNOLOGY, **27**(2), pp. 129–159, 1992

REVIEW

Hydrodynamic Modeling of Droplet Coalescence at Liquid–Liquid Interfaces

WOLFGANG ROMMEL
CHAIR A FOR CHEMICAL ENGINEERING
TECHNICAL UNIVERSITY OF MUNICH
ARCISSTRASSE 21, D-8000 MUNICH 2, GERMANY

WALTER MEON
DAGUSSA AG
ABT. VTC-IM, D-8450 HANAU/WOLFGANG, GERMANY

ECKHART BLASS
CHAIR A FOR CHEMICAL ENGINEERING
TECHNICAL UNIVERSITY OF MUNICH
ARCISSTRASSE 21, D-8000 MUNICH 2, GERMANY

Abstract

Liquid–liquid dispersions consisting of a dispersed and a continuous liquid which are mutually unsoluble or at least almost unsoluble occur in many separation processes. On the one hand they are intentionally produced to achieve a high surface area per unit volume for heat and/or mass transfer, e.g., in the case of the solvent extraction. On the other hand such dispersions sometimes occur unintentionally, for instance, during the condensation of a heteroaceotropic mixture or in the frame of wastewater treatment, e.g., after oil accidents. Under almost all circumstances, the dispersions have to be separated into their clear homophases. Simple gravity settlers without any coalescing aids are applied in most cases for this purpose. Within such apparati the drops flow together ("coalesce") and form a coherent phase. This review discusses the physical models of gravity settlers. Calculation methods for the coalescence of single droplets and for the coalescence of droplet swarms in dense dispersions are reviewed. Finally, possibilities and limitations of hydrodynamic settler modeling are pointed out.

1. INTRODUCTION

The separation of liquid–liquid dispersions in gravity settlers without coalescing aids is governed by the interaction of various effects (*1*). Up to

now a complete physical description of gravity settlers has been impossible because several effects involved are nonquantifiable. Therefore, the design of settlers requires extensive experimental work. On the other hand, industry is interested in simple methods for a reliable prediction of the separation process in gravity settlers.

The coalescence of drop swarms in horizontal and vertical, batchwise, and continuously operated settlers has been intensively investigated during the last 25 years. Different mathematical models for separation at a horizontal liquid–liquid interface have been developed. One can distinguish two major groups: The so-called "deterministic models" focus on the drainage of a thin layer between drop and interface or between two neighboring drops as the governing process of coalescence in a dense-packed dispersion. The so-called "probability models" consider the separation to be a stochastic process and try to simulate it under the assumption of distinct probabilities of drop–drop coalescence ("ddc," binary coalescence) and drop–interface coalescence ("dic," interfacial coalescence). Every author has fitted his model to the specific boundary conditions of his experiments. Among other things, this review intends to examine whether these models can be applied to different boundary conditions.

2. COALESCENCE OF SINGLE DROPS AT HORIZONTAL INTERFACES

The complex interactions of various influencing effects make the coalescence in a gravity settler seem to be a stochastic process, because there is little knowledge available on these effects and their interference. Fundamental principles of interface physics, chemistry, and colloid science that could be adopted for the engineering treatment of the coalescence process are missing. The first step to the theoretical calculation of settlers is an examination of the coalescence of a single droplet at a planar interface.

2.1. Coalescence Process

According to Fig. 1, we can distinguish among three succeeding steps of the coalescence process at a principle interface (*2*):

1. The drop approaches the interface, is decelerated, and occasionally oscillates moderately. Drop and interface deform.
2. Drop and interface enclose a thin layer of continous phase which has to drain to a critical low thickness. During the drainage the drop apparently rests at the interface.
3. Finally, the thin layer ruptures and the drop can flow into its mother phase. This flow-in process is often not completed and a secondary drop remains. We call this "partial coalescence."

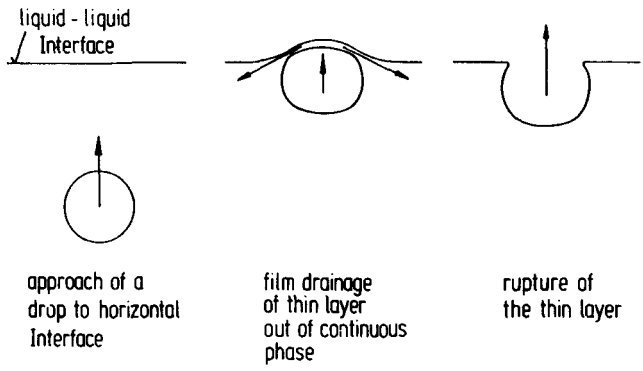

FIG. 1. Course of the coalescence process of a single droplet at a plain interface.

The time-determining step of the whole coalescence process is the drainage of the thin layer. It governs the *time of coalescence* which characterizes the coalescence process. Many examinations focus on this drainage process. Its physical nature is phenomenological because it cannot be modeled mathematically. Hartland (*3*) reports that the thickness of the draining layer shows a maximum in the middle of the drop which is degraded by the flowing out of the continuous phase. This process is called "dimpling." At the contact edges a minimum thickness of the layer forms; it is called "barrier ring" (see Fig. 2).

Originally, Hartland attributed this fact to circulation inside the drop, but he later detected the same effect during examinations of solid spheres. Hodgson and Woods (*4*) focused on the influence of surface-active agents on coalescence and found that an increasing concentration of surfactants or the growing age of the interface amplifies the occurrence of dimpling. They attributed this fact to a backflow of the continuous phase into the thin layer, which is caused by gradients of the interfacial tension. Figure 3 shows that the reason for backflow, namely, the gradients of surfactants concentration, is induced by the drainage process itself.

The Marangoni backflow into the draining layer leads to higher coalescence times and a strong scattering of these times. Very low amounts of contamination, such as are evident even in highly purified technical liquid systems, suffice to cause dimpling. That means that coalescence is always connected with a dimpling effect! Furthermore, Hodgson and Woods (*4*) showed that the contents of draining liquids within the barrier ring remain almost constant after the backflow during the approach of the drop toward the interface. This fact is attributed to rigid interfaces at the barrier ring. Therefore, the drop approaches the interface only at the barrier ring while

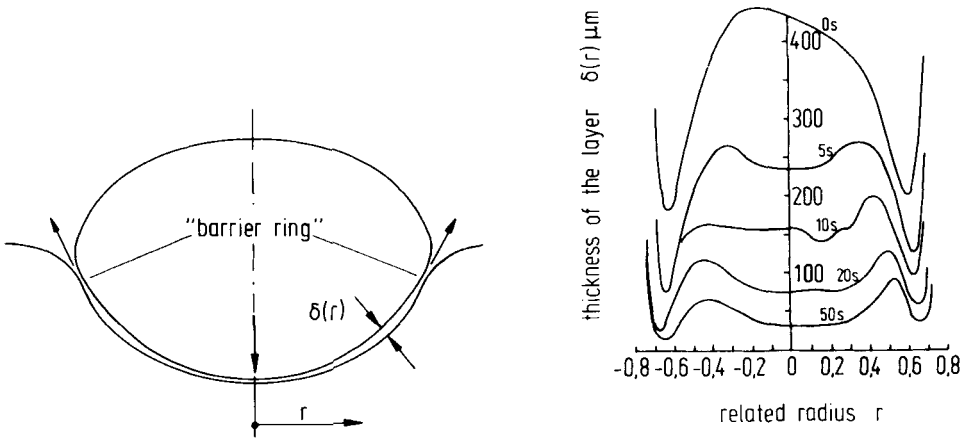

FIG. 2. Thickness of the enclosed thin layer under a glycerol drop in liquid paraffin according to Hartland (*3*).

its radius increases. Closer considerations include the interfacial viscosity and elasticity. The momentary state-of-the-art was reviewed by Wasan and Malhotra (*5*). However, the statements are theoretical only, without any experimental proof.

Knowledge concerning electrostatic and -kinetic influences on the coalescence is restricted to the general proposition that the formation of repulsing double layers hinders droplet approach. There are no models which take this fact into account for the calculation of the thin liquid layer between drop and interface. Chen, Hahn, and Slattery (*6*) recently published a

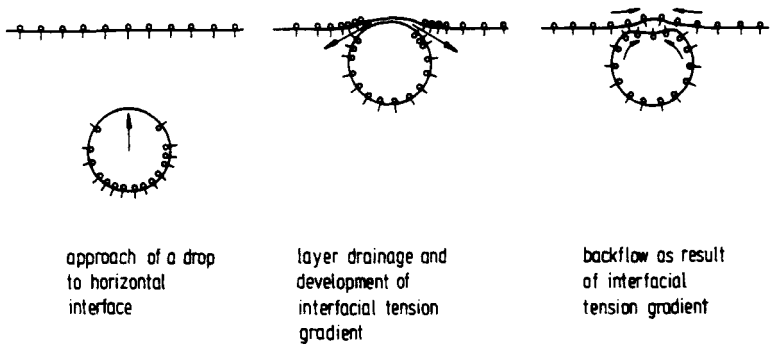

FIG. 3. Hinderance of the drainage process and backflow due to a gradient of the interfacial tension.

formulation for future modeling attempts, but, so far, it has had no practical validity.

Mass transfer between the phases also exhibits a strong influence on the coalescence process. Nowadays, only a qualitative estimation of whether coalescence is favored or hindered is possible.

On the contrary, interparticular interactions depending on the van-der-Waals forces have been described in global numbers like the Hamaker or London-Hamaker constant, and in this way they are accessible for physical modeling of the coalescence process.

The hydrodynamic effects, i.e., the pressing of drops against the draining thin layer and the flowing of a Newtonian liquid in an irregularly shaped duct, can be modeled by using well-known hydrodynamic principles.

2.2. Models of Coalescence

As mentioned before, the drainage of the thin layer governs the coalescence process and is affected by all the effects described above. The time of coalescence, which is the difference in time between the moment a drop reaches the principle interface and its coalescence, is a measure for the drainage process. Balance models proposed by Hartland (*8*) and others require knowledge of this parameter.

Most coalescence models either calculate the time of drainage of a thin layer between two approaching interfaces until rupture or the approaching velocity between two drops or a drop and a plain interface. They have been reviewed in various papers (*9–11*, *13*, *14*, *72*). In addition, there are some models that use dimensional analysis to evaluate the time of coalescence (*15–17*). All models employing steady-state symmetrical drainage of the thin layer are based on hydrodynamic principles. Some recent models involve intermolecular interactions within the thin layer by incorporating the Hamaker coefficient.

The following paragraphs describe calculation results for the models listed in Table 1 with experimental data of Pabst (*72*), Charles and Mason (*18*), Lawson (*19*), Gillespie and Rideal (*20*), Lang and Wilke (*21*) and Jeffreys (*15*, *16*) for toluene drops in water.

One of the earliest models was the "disc-model" of Charles and Mason (*18*). They computed the critical thickness of the thin layer by putting measured coalescence times into their model formulation. The model is based on two parallel and circle-shaped discs with rigid surfaces which approach each other. The discs correspond to the contact area of the drop with the interface. The radius of the contact area r_f is determined according to Derjaguin and Kussakov (see Refs. *22* and *23* and Table 1). This equation was proved by the work of Princen (*24*, *25*) and was used in recent papers

TABLE 1
Survey of Models of the Coalescence of Single Droplets at Plain Interfaces

author	theory		time of coalescence
Charles G.E. Mason S.G. [18]	drainage between two parallel discs with rigid interfaces "Parallel - disc - model"	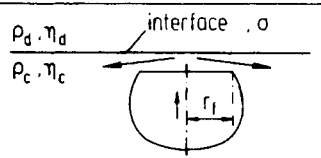	$t_k = \frac{\eta_c}{4} \cdot \left(\frac{\Delta\rho \cdot g \cdot (d_p/2)^5}{\sigma^2}\right) \cdot \left(\frac{1}{\delta_c^2} - \frac{1}{\delta_1^2}\right)$
Hodgson T.D. Woods D.R. [4]	drainage under a cylinder outside of the "barrier ring", rigid interfaces $\delta_c = \left(\hat{H}_{c,d} \cdot \left(\frac{d_p}{2 \cdot \sigma}\right)\right)^{1/4}$	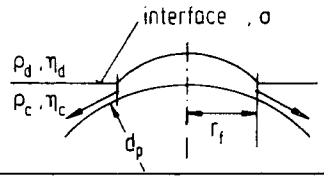	$t_k = \frac{3}{2} \cdot \frac{\eta_c \cdot d_p^2}{\sigma} \cdot \left(\frac{1}{\delta_c} - \frac{1}{\delta_1}\right)$
Lang S.B. Wilke C.R. [21]	drainage under a sphere with rigid interfaces δ_c from Hodgson /hod 69b/ Θ from Princen /pri 69/	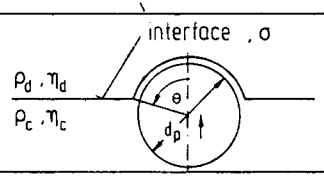	$t_k = \frac{6 \cdot \eta_c \cdot (d_p/2)^3}{\sigma} \cdot I(\Theta) \left(\frac{1}{\delta_c^2} - \frac{1}{\delta_1^2}\right)$ $I(\Theta) = \frac{\cos\Theta - 1 - (4 \cdot \ln\cos(\Theta/2))}{\sin^2\Theta}$
Buevich Yu.A. Lipkina E.Kh. [26]	droplet approach at the "barrier ring" (see /hod 69b/) Van der Waals forces evaluated by the London - Hamaker coefficient	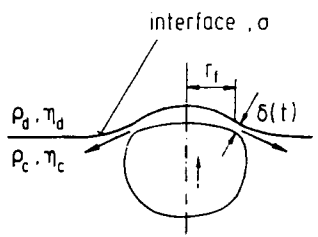	$t_k = 0{,}294 \cdot \frac{n^2 \cdot \eta_c \cdot r_f \cdot (d_p/2)}{\sigma^{0.6} \cdot \hat{H}_{c,d}^{0.4}}$
Chen J.D. Hahn P.S. Slattery J.C. [23]	$\hat{H}_{c,d} = 1{,}13 \cdot 10^{-28}\ N \cdot m^2$ radius at the "barrier ring" r_f $r_f = d_p^2 \cdot \left(\frac{\Delta\rho \cdot g}{12\,\sigma}\right)^{1/2}$		$t_k = 0{,}45 \cdot \eta_c \cdot d_p \cdot \hat{H}_{c,d}^{-0.4} \cdot \left(\frac{d_p^4 \cdot \Delta\rho \cdot g}{12\,\sigma^2}\right)^{0.6}$ (condition : $\delta_c > 4000\,A^\circ$)

concerning coalescence, e.g., that of Chen, Hahn, and Slattery (*23*). Hodgson and Woods (*4*) realized well-defined interfacial conditions for the coalescence process by applying a special cleaning device. This enabled them to conduct reproducible coalescence experiments for the first time. They observed that after the formation of a barrier ring, the approach process takes place only at the barrier ring and the liquid content remains enclosed within this ring. Figure 4 illustrates this observation. Based on this fact, they developed their "cylinder model" for the computation of coalescence times. It describes the drainage between the lateral area of a horizontal cylinder and a plain interface in a simplified way in which only the flow region outside the barrier ring is taken into account. The model of Lang and Wilke (*21*) regards the coalescence process as the drainage of a thin layer of equal thickness below a ball-shaped drop with a rigid surface. They also calculated the critical thickness by using measured times of coalescence. The model of Chen, Hahn, and Slattery (*23*) is based on theoretical considerations by Buevich and Lipkina (*26*). It takes the attracting pressure of van der Waals into account by applying the Hamaker coefficient $H_{c,d}$.

Figure 5 shows a comparison between computation results of the reviewed models and experimental data for the coalescence times of single drops. The values of critical thickness δ_c have been calculated according to Vrij and Overbeek (*27*) and of the drop shapes according to Princen (*25*). The experiments exhibit increasing times of coalescence with growing drop diameters. From the hydrodynamic point of view, this fact is due to the increasing contact area between the drop and the interface, which slows down the drainage process. Wasan and Malhotra (*5*) pointed out that it is

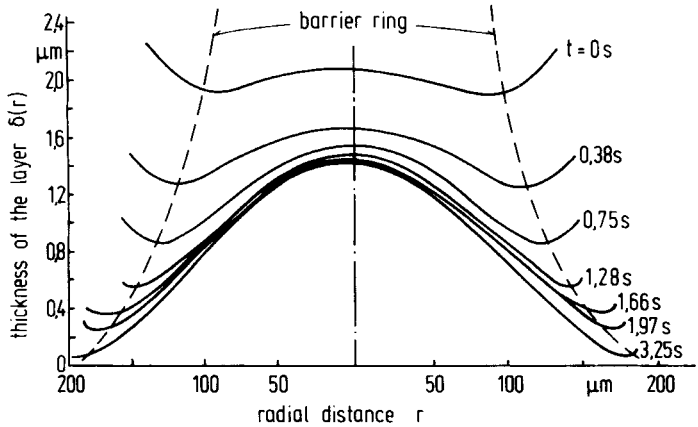

FIG. 4. Time-dependent course of the thickness of the layer between an anisol droplet in water with sodium dodecyl sulfate according to Hodgson and Woods (*4*).

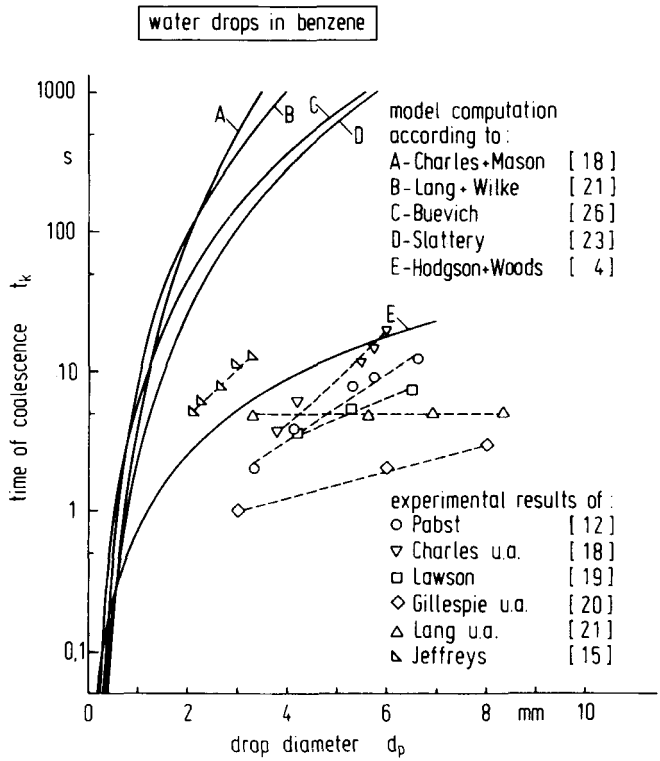

FIG. 5. Comparison of computed and measured times of coalescence of water droplets in benzol.

obvious that hydrodynamic models rate this effect too high. Besides, all models take only the symmetric drainage processes into account. In reality, drainage is unsymmetric and therefore faster. These facts explain the higher values of the computed times compared to the measured ones. All experimental results are affected by the influence of surfactants, by electric effects, and partly by mass transfer when they are based only on hydrodynamics. It is interesting that the simplest model of Hodgson and Woods (*4*) shows the best correlation between computed and measured data.

3. COALESCENCE OF DROP SWARMS AT HORIZONTAL INTERFACES

Research on single drops should provide the basis for theoretical modeling of the coalescence of drop swarms in liquid–liquid dispersions. How-

ever, no way was found to transfer the results appropriately. Therefore, the coalescence of drop swarms at horizontal interfaces in liquid–liquid dispersions was investigated independently from the single drop considerations reviewed in the previous section. Table 2 provides a survey on most of these investigations. They have been prevailingly done in an empirical manner. The physical model formulations are either based on monolayers or on multilayers of ball-shaped or deformed particles at the interface. According to Lawson (*19*), the coalescence of monolayers is strongly influenced by disturbances like vibration, pressure impact, and shock from outside, which lengthens the time of coalescence compared to single drops. Robinson and Hartland (*28*), in contrast to Lawson, report that the dense packed drops of a two-dimensional monolayer coalesce faster than do single drops. The reason is that drainage of the thin layer between a drop of the monolayer and its mother phase occurs faster because of the lower depth of immersion of the drop and the smaller amount of enclosed continuous phase. Davies, Jeffreys, and Smith (*17*) found that the time of coalescence in monolayers is inverse proportional to the number of drops related to the unit of time. The inconsistent results of investigations of coalescence in monolayers do not allow for any conclusion on the separation performance of dense dispersions. Therefore, most authors focus on multilayers of drops, i.e., dense-packed dispersions, and investigate the structure of the dispersion band in order to gain information on the coalescence process.

3.1. Structure of the Dense Dispersion

Hitit (*29*), Allak and Jeffreys (*30*, *31*) and Barnea and Mizrahi (*32*, *33*) distinguish two different regions within the dense-packed zone. Hitit, Allak, and Jeffreys name them "floculation," "packing," and "coalescence zone." Figure 6 schematically illustrates such a dispersion band in a vertical settler. The floculation zone (I) is the immediate entrance region of the drops into the dispersion band. No coalescence takes place, but the drops arrange themselves in order by a slow sedimentation motion. The hold-up rises erratically from its entry value of about 10% up to about 50%. It further rises within the packing zone slowly up to about 75%, which corresponds to the hold-up of a dense-packed bed of spheres with equal diameter. The drops grow by drop–drop coalescence (ddc) and adapt their shape to their immediate environment. According to Allak and Jeffreys (*30*, *31*), the packing zone covers most of the dense dispersion. Again, the hold-up rises erratically up to almost 100% with decreasing distance from the principle interface which separates the dispersion region from the clear mother phase of the drops. The packing zone shifts to the coalescence

TABLE 2
Survey of Models of the Coalescence of Drop Swarms at Plain Interfaces

author(s)	lit.	remarks	resulting equations	
			discontinuous settling process	continuous settling process
Ryon, Daley, Lowrie (59-63)	[67] [42] [43]	horizontal settler with dispersion band mixer experimental mixer settler investigations with empirical correlation of results	$v_{d,stat} = \frac{\varepsilon_d h_{00}}{t_{stat}} = \frac{\varphi_v h_{00}}{t_{stat}}$	$H_D = c \cdot \left\lvert \frac{\dot{V}_d}{A} \right\rvert^y$ $1{,}4 < y < 11$
Gondo, Kusunoki (69)	[68]	horizontal settler with dispersion band mixer experimental mixer settler investigations with empirical correlation of results		$H_D = c \cdot n_M^{2.8} \cdot \varepsilon_d^{4.9} \cdot \left\lvert \frac{\dot{V}}{A} \right\rvert^{3.1}$ with $\left\lvert \frac{\dot{V}}{A} \right\rvert = \left\lvert \frac{\varepsilon_d \dot{V}_d}{A} \right\rvert$
Davies, Jeffreys, Ali (70-71)	[69] [17]	horizontal settler with dispersion wedge mixer physical model with empirical correlation of parameters		$\frac{\dot{V}_d}{D} = 2 \cdot \varphi_1 \cdot v_D \left[\left(d_P^{3/2} + \frac{L_D}{4 \cdot v_D \cdot f_0} \right)^{2/3} - d_{PO} \right]$ with $f_0 = 1{,}32 \cdot 10^5 \left(\frac{L_D}{d_P} \right)^{0.18} \cdot \left(\frac{d_P^2 \Delta \rho g}{\sigma} \right)^{0.32}$
Smith, Davies, Jeffreys, Ali (70-71)	[70] [17]	vertical settler with dispersion band spray tower equilibrium model with empirically correlated SDIC- and DDC times		$\frac{H_D}{d_{PO}} = c \cdot \left(\frac{\dot{V}_d \cdot \eta_c}{\sigma} \right)^{y_1} \left(\frac{d_{PO}^2 \Delta \rho g}{\sigma} \right)^{y_2} \left(\frac{\eta_d}{\eta_c} \right)^{y_3}$

Hosozawa, Suzuki, Tadaki, Maeda (73)	[64]	vertical settler with dispersion band spray tower statistic model with DDC- and SDC probabilities (Monte- Carlo simulation) empirical correlation of experimental results		$H_D = c \cdot \left(\frac{\dot{V}_d}{A}\right)^y$ $1{,}2 < y < 5{,}8$
Allak, Jeffreys (74)	[71] [30] [31] [72]	vertical settler with dispersion band spray tower empirical correlation of experimental results by a dimension analysis		$\left(\frac{\vartheta_R \sigma}{\eta_c H_D}\right) = 11{,}22 \cdot \left(\frac{d_{32}}{H_D}\right)^{-0{,}331} \cdot \left(\frac{\Delta\rho g H_D^2}{\sigma}\right)^{-0{,}267} \cdot \left(\frac{\eta_c \dot{V}_d}{\sigma}\right)^{-0{,}768}$
Doulah, Davies (74)	[7]	- - probability model, computer simulation by means of Monte- Carlo method		$H_D = c_1 \exp\left(c_2 \frac{\dot{V}_d}{A}\right)$
Slater, Ritcey, Pilgrim (74)	[47]	horizontal settler with dispersion wedge mixer empirical correlation for batch settling process with model theory for the transfer to continuous settlers	$t_{stat} = -35{,}38 - 32{,}6 \cdot \log\left(\frac{V_c}{V_d}\right) + 24{,}8 \cdot \log(t_M + 20) + 11{,}5 \cdot \log(n_M - 165)$ $v_{c,stat} = w_{r\infty} \cdot (1 - \varepsilon_d)^n$ $n = 4{,}65$ $Ar < 18$ $n = 5{,}5 \cdot Ar^{-0{,}06}$ $18 < Ar < 5 \cdot 10^6$ $n = 2{,}2$ $5 \cdot 10^6 < Ar$	$\dot{V}_d = v_{c,stat} \cdot 2\frac{\varepsilon_d}{(1-\varepsilon_d)}$
Barnea, Mizrahi (75)	[32] [33] [45] [46]	horizontal settler with dispersion band mixer experimental mixer settler investigations with empirical correlation of results	$\left(\frac{V}{A}\right)_N = c \cdot t_{stat}^{-y}$	$H_D = c \cdot \left(\frac{\dot{V}_d}{A}\right)^y$ $1{,}4 < y < 11$

(*continued*)

TABLE 2 (continued)

Stönner, Wöhler (75)	[73]	horizontal settler with dispersion band mixer empirical correlation of own experimental datae and those taken from literature		$H_D = \frac{c_2(V_d/A)}{c_1(c_2+(V_d/A))}$
Vijayan, Ponter (76)	[74]	horizontal settler with dispersion wedge mixer physical model with parameters τ_D, τ_{DI} determined from experimental datae		$v_D \frac{d[n(l)]}{d\,l} = -n(l)\left(\frac{1}{\tau_{DI}} + \frac{1}{2}\frac{1}{\tau_D}\right)$ $\frac{d(d_P)}{d\,l} = \frac{1}{6}\cdot\frac{d_P}{v_D\tau_D}$
Drown, Thomson (77)	[75]	horizontal settler with dispersion wedge spray tower empirical correlation only to calculate the inflow-length		$L_{D;S} = 1{,}7\cdot\left[\frac{D_{iS}}{\sqrt{g}}\right]\bar{v}^{0.5}\cdot v_{iS}$
Vieler, Glasser, Bryson (77)	[34]	- - empirical correlation to calculate H_D identical with the equation of Stönner, Wöhler		$H_D = \frac{c_2(V_d/A)}{c_1(c_2+(V_d/A))}$
Godfrey, Chang-Kakoti Slater (77)	[35]	horizontal settler with dispersion band mixer empirical correlation identical with the equation of Ryon and others respectively		$H_D = c\cdot\left[\frac{V_d}{A}\right]^y$ $\quad 1{,}4<y<11$
Golob, Modic (77)	[49]	horizontal settler with dispersion band mixer empirical correlation for the coherence between batch experiment and continuous settler. Results identical with the equation of Ryon, Barnea, Mizrahi, Godfrey and others		$H_D = c\cdot\left[\frac{V_d}{A}\right]^y$ $\quad 1{,}4<y<11$

Hartland, Vohra (78)	[8]	vertical settler with dispersion band spray tower physical model of empirically determined parameters τ_D, τ_{DI}		$H_D = 6 \cdot \frac{\dot{V}_d \tau_D}{\varepsilon_d} \cdot \ln\left[\frac{3 \dot{V}_d \tau_D}{2 \varepsilon_d d_{PD}}\right]$
Kumar, Vohra Hartland (80)	[76]	vertical settler with dispersion band spray tower physical model of empirically determined parameters τ_D, τ_{DI}, ε_d, ε_{di}	$h_D = h_{D0} - \frac{4 \varepsilon_{di} d_{PD} \tau_D}{\varepsilon_d \cdot \tau_{DI}} \cdot \left\{\exp\left[\frac{t}{6\tau_D}\right] - 1\right\}$ $t_{stat} = 6 \cdot \tau_D \ln\left[1 + \frac{\varepsilon_d \tau_{DI} h_{D0}}{4 \varepsilon_{di} d_{PD} \tau_D}\right]$ for $\tau_D \to \infty \gg \tau_{DI}$ $t_{stat} = \frac{3 \varepsilon_d \tau_{DI} h_{D0}}{2 \cdot \varepsilon_{di} d_{PD}}$	$w_{rs} = -22{,}642 \cdot \frac{\eta_c}{d_{PD} \cdot \varrho_c} + \frac{1}{2} \cdot \left[(45{,}283 \frac{\eta_c}{d_{PD} \cdot \varrho_c})^2 - 10{,}064 \cdot \left(\frac{1-\varepsilon_d}{1+4{,}56 \varepsilon_d^{0{,}73}}\right) \cdot d_{PD} g \frac{\Delta\varrho}{\varrho_c}\right]^{\frac{1}{2}}$ with $w_{rs} = \frac{\dot{V}_d}{\varepsilon_d} + \frac{\dot{V}_c}{1-\varepsilon_d}$ $0{,}01 < \varepsilon_d < 0{,}76 \qquad 0{,}16 < Re_{rs} < 3169$
Gomez, Wilkinson (80)	[77]	resulting equation, identical to those of Ryon and others like Barnea, Mizrahi, Godfrey, Golob, Modic		$H_D = c \cdot \left(\frac{\dot{V}_d}{A}\right)^y$
Reissinger, Schröter, Bäcker (81)	[59]	horizontal settler with dispersion wedge empirical model with parameters taken from industrial practice	$t_{dyn} = c \cdot t_{stat}$	$L_D = \frac{\dot{V} t_{dyn}}{A}$
Austin, Jeffreys (81)	[51]	horizontal settler with dispersion wedge mixer experimental mixer settler studies with empirical correlation of results	$\frac{h_D}{h_{D0}} = c_1 \cdot \exp(-c_2 t)$	$L_D = c \cdot \left(\frac{\dot{V}_d}{b}\right)^{3/2}$

(*continued*)

TABLE 2 (*continued*)

Hartland (81)	[60] [61]	vertical settler physical model for the growth of the dispersion band of empirically determined parameters y, τ_{DI}, τ_{DI}	for $t_{stat} > \tau_D$ $\ln\left(\frac{h_{00}}{h_0}\right) = \left[\ln\left(\frac{h_{00}}{h_{00_p}}\right) - \frac{2\varepsilon_{dI} t_{w_p}}{3\varepsilon_d \tau_{DI}'}\right] + \left(\frac{2\cdot\varepsilon_{dI}}{3\cdot\varepsilon_d\tau_{DI}'}\right) t$ for $\tau_{DI}' = \tau_{DI}$ $\ln\left(1-\frac{h_0}{h_{00}}\right) = \left[-\ln\left(\frac{\varepsilon_d h_{00}\tau_{DI}'}{4\cdot\tau_D\cdot d_{PD}\varepsilon_{dI}}\right)\right] + \left(\frac{1}{6\tau_D}\right)\cdot t$	$H_D = 6c\frac{\dot{v}_d^{y-1}}{\varepsilon_d}\ln\left(\frac{3\cdot\dot{v}_d\tau_{DI}}{2\varepsilon_{dI}d_{PD}}\right)$
Stönner, Wiesner (82)	[78]	horizontal settler with dispersion band mixer theoretical equilibrium model with empirically correlated parameters x_{10}, c_1, c_2	$\frac{dh_0}{dt} = -c_2\left[1-\frac{h_{00}}{h_0}x_{10}\exp(-c_1 t)\right]$	$H_0 = \frac{x_{10}c_2\cdot(\dot{V}_d/A)}{c_1(c_2+(\dot{V}_d/A))}$ with $\frac{\dot{V}_d}{A} < \frac{\dot{V}_{d\,max}}{A} = \frac{c_1 H_A}{1+x_{10}}$
Weiß (82)	[53]	only for discontinuous settler empirical correlation of Batch results	$\dot{v}_{d,stat} = \frac{\varepsilon_d h_{00}}{t_{stat}} = \frac{\varphi_v h_{00}}{t_{stat}}$	
Hossain, Sarkar, Mumford, Phillips (83)	[65]	horizontal settler with dispersion wedge mixer empirical correlation of experiment results (dimensionanalysis)		$\frac{L_D}{L_A} = 3{,}3\cdot10^{-7}\left(\frac{\varrho\dot{V}_d D}{\eta}\right)^{1{,}17}\cdot\left(\frac{\dot{V}_d}{\dot{V}_c}\right)^{0{,}08}\cdot\left(\frac{d^3 n_M^2\varrho_c}{\sigma}\right)^{0{,}65}\cdot\left(\frac{D}{D-D_w}\right)^{-0{,}49}$

Jeelani, Hartland (85)	[37] [39] [40]	horizontal settler with dispersion band mixer balance model with empirically determined parameters τ_D, k_1, k_2	$t = \frac{1}{K_1} \cdot \ln\left(\frac{h_{D0}}{h_D}\right) + \frac{1}{K_2} \cdot (h_{D0} - h_D)$ with $K_1 = c_1 \left\lvert \frac{2 \cdot \varepsilon_{dI} d_{PO}}{3 \cdot \tau_{DI}} \cdot \frac{\gamma_1}{\varepsilon_{iS} \cdot h_{D0}} \right\rvert$ $K_2 = c_1 \left\lvert \frac{2 \varepsilon_{dI} d_{PO}}{3 \cdot \tau_{DI}} \cdot \frac{\gamma_1}{\varepsilon_d c_2} \right\rvert$	$H_D = \frac{\left\lvert \frac{3 \cdot \dot{v}_d \cdot \tau_{DI}}{2 \cdot \varepsilon_{dI} \cdot d_{PO}} \right\rvert \cdot h_{D0}}{K_1 \gamma_1 - \left\lvert \frac{3 \cdot \dot{v}_d \cdot \tau_{DI}}{2 \cdot \varepsilon_{dI} d_{PO}} \right\rvert \cdot K_2 \cdot \frac{\varepsilon_d}{\varepsilon_{iS}}}$ with $\varepsilon_{iS} = \frac{V_d}{V_c + V_d}$ $\gamma_1 < 1$ for deformable drops $\gamma_1 = 1$ for rigid drops
Siemons (85)	[56]	horizontal settler with dispersion wedge - physical model with empirically adapted parameters c_1 to c_4	$\frac{dh_D}{dt} = -\frac{2}{3} \cdot \frac{\varepsilon_{dI}}{\varepsilon_d} \cdot \frac{d_{PO}}{c_1 c_2 h_D d_{PO}^{c_4} + (c_3 c_4)/h_D}$ $\frac{d(d_P)}{dt} = \frac{d_P}{6(c_1 h_D d_P^{c_4} + c_2 h_D)}$	$H_D = H_{D0} - \frac{1}{3} \cdot \frac{\varepsilon_{DI} H_{D0}}{v} \cdot \int_0^{L_a} \left\lvert \frac{d_{PO}}{c_1 c_3 H_D d_{PO}^{c_4} + c_2 c_4 / H_D} \right\rvert dz$
Löbmann, Blaß (85)	[57]	vertical settler with dispersion band mixer empirical correlation of Batch data by dimension analysis, analytically solvable	$v_{d,stat} = \frac{\varepsilon_d \cdot h_{D0}}{t_{stat}} = \frac{\varphi_v h_{D0}}{t_{stat}}$ $Ar^{1/3} = 11{,}71 \cdot (Re \cdot Fr')^{0.305}$ $Ar = d_{32}^3 \cdot \frac{\varrho_c^2 g}{\eta_c^2} \cdot \frac{\lvert \Delta\varrho \rvert}{\varrho_c}$ $Re \cdot Fr' = v_{d,stat}^3 \cdot \frac{\varrho_c}{g \cdot \eta_c} \cdot \frac{\varrho_c}{\lvert \Delta\varrho \rvert}$	

(continued)

TABLE 2 (*continued*)

Misek (86)	[79]	horizontal settler with dispersion band - physical model with empirically correlated parameters c_0, c_r, c_x		$H_D = \frac{v_d}{a \cdot (1 - b \cdot v_d)}$ $a = \frac{d_p \cdot \varepsilon_{dI} \cdot \bar{\varepsilon}_d \cdot \Delta\rho \cdot g}{c_c \cdot \eta_c}$ $b = \frac{c_f \cdot \eta_c}{\Delta\rho \cdot g \cdot d_p^2 \cdot (1 - \varepsilon_{dI})^2}$ $c_f = 24{,}2 \pm 5\%$ $c_c = 6930 \div 24948$
Jeelani, Hartland (86)	[38]	**vertical settler with dispersion band** **spray tower** physical model with correlations of experimental results of other authers		$\frac{d_{pI}}{d_{p0}} = 0{,}5 \cdot \left(\frac{\Delta\rho}{\rho_c}\right)^{0{,}265} \cdot \left(\frac{v_d}{c \cdot g}\right)^{0{,}098} \cdot \left(\frac{\rho_c^2 \cdot \sigma^3}{\Delta\rho \cdot g \cdot \eta_c^4}\right)^{0{,}123} \cdot \left(\frac{\eta_c}{\eta_d}\right)^{-1{,}614}$ $\varepsilon_0 = 0{,}21 \cdot \left(\frac{v_d^2}{c \cdot g}\right)^{-0{,}173} \cdot \left(\frac{d_{p0}}{c}\right)^{0{,}534} \cdot \left(\frac{\eta_c}{\eta_d}\right)^{0{,}607}$ with $c = \left(\frac{\sigma}{\Delta\rho \cdot g}\right)^{0{,}5}$
Shen, Shen (86)	[80]	horizontal settler with dispersion band **mixer** enlarging of Hartland's and Vohra's model: τ_b, τ_i only dependent of d_p; d_p from empirical correlation of stirring conditions		$H_D = c_1 \cdot \left(\frac{\dot{V}_d}{A}\right)^{p-1} \cdot n_M^{1{,}2m} \cdot \ln\left[c_2 \cdot \left(\frac{\dot{V}_d}{A}\right) \cdot n_M^{1{,}2(1-m)}\right]$

Gourdon, Muratet, Casamatta (86)	[81]	vertical settler with dispersion band (sieve tray on the principal interface) spray tower statistic collision model with empirically matched DDC- frequence DIC not relevant (sieve tray)		
Jiang Yu, Sun, Zhao (86)	[82]	horizontal settler with dispersion wedge mixer physical calculating model with empirically adapted parameters		resulting equations too large for this table (see /jia 86/)
Dalingaros, Hartland	[83]	vertical settler with dispersion band drop column combination between physical models, dimension analysis and empiric datae		$H_0 = \frac{K}{g} \cdot \left(\frac{\sigma}{\Delta\rho \cdot g}\right)^{1/2} \cdot \frac{1}{\overline{d_{p0}}} \cdot \left(\frac{\dot{V}_d}{\bar{\varepsilon} \cdot A}\right)^2$ with $25000 \leq K \leq 30000$
Hartland, Jeelani (87)	[36]	vertical settler with dispersion band mixer physical model for the coherence between Batch- experiment and continuous settler		$H = \left(\frac{1}{k_1}\right)^{p(1-i)} \cdot \frac{1}{\bar{\varepsilon}} \cdot \left(\frac{\dot{V}_d}{A}\right)^{1+p/(1-i)}$

(*continued*)

TABLE 2 (*continued*)

Jeelani, Hartland	[84]	horizontal settler with dispersion wedge mixer combination of physical model and empiric		empiric correlations: $\tau_{i0} = \frac{66{,}5 \cdot Bo^{-0{,}21}}{\sqrt{g/d_{p0}}}$ (± 15 %) $\tau_{b0} = 48{,}2 \cdot Bo^{-0{,}7}$ (± 35 %) $T = 428 \cdot Bo^{-0{,}585}$ (± 20 %) with $Bo = \frac{\Delta\rho \cdot g \cdot d_{p0}^2}{\sigma}$ length of dispersion wedge: $L_0 = \frac{3}{2} \cdot \frac{\dot{V}_d \cdot \tau_{i0}}{d_{p0}}$ $H_{00} = \frac{\dot{V}_d}{\bar{\varepsilon}} \cdot \frac{T}{L_0} \cdot \sqrt{g/d_{p0}}$
Sklokin, Leif, Masloboyeva	[86] [85]	horizontal and vertical settler - further developed model of the model of Stoenner et. al. using empiric formulations		$H_0 = \frac{\frac{\dot{V}_d}{\dot{V}_{d,grenz}}}{1 - \frac{\dot{V}_d}{\dot{V}_{d,grenz}}} H_{1/2}$ empiric formulation for $\dot{V}_{d,grenz}$ a. $H_{1/2}$: $\frac{\dot{V}_{d,grenz}}{A} \cdot \frac{\eta_c}{\sigma} = C \cdot \left(\frac{\Delta\rho \cdot g \cdot d_{p0}}{\sigma}\right)^n$ $C = 3{,}0 + 5{,}3 \cdot 10^3 \cdot \left(0{,}2 - \frac{\Delta\rho}{\rho_c}\right)^{2{,}9}$ $n = 0{,}47 + 88{,}2 \cdot \left(0{,}2 - \frac{\Delta\rho}{\rho_c}\right)^{3{,}0}$ $H_{1/2} = 0{,}05\,m \div 0{,}10\,m$

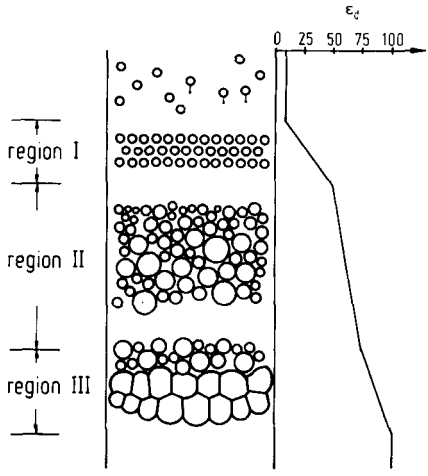

FIG. 6. Schematic illustration of a dense dispersion band in a vertical settler when the heavier liquid is the dispersed one.

zone (III) which has a thickness of only about one or two times that of the drop diameter. There exist only strongly deformed drops which are densely pressed together and exhibit the structure of dodecaders within this zone. These deformed drops flow into the clear mother phase by drop–interface coalescence.

By referring to their measured hold-up values of the dispersion band, Barnea and Mizrahi (*32*) distinguished only two different regions. The first region covers the flocculation and packing zone of Hitit, Allak, and Jeffreys; the second one corresponds to the coalescence zone of these authors. The difference between the two points of view can be attributed to the different experimental boundary conditions. Hitit, Allak, and Jeffreys carried out their experiments in a spray column with a relatively low hold-up of about 10%, while Barnea and Mizrahi used a mixer-settler which exhibited starting values for the hold-up of between 30 and 50%. These high starting hold-ups made it impossible to detect the flocculation zone.

All the authors agree that drainage of the continuous phase through the packing zone governs the steady-state height of the dense dispersion band. In addition, Hitit (*29*) reported that the height of the dispersion band depends strongly on the size of the drops entering it.

Apart from this classification of different zones within (real) multilayer dispersion bands, Doulah and Davies (*7*) and Hartland and Vohra (*8*) proposed the dispersion of equally sized drops within the entire dispersion band. Batch experiments conducted in mixers exhibit this idealized con-

dition for a short time after stopping intensive mixing. However, the dispersion quickly adopts the multizone structure proposed by Barnea and Mizrahi in the course of the settling process. The dispersion band decays as long as only a monolayer is present (*19*, *28*), which unites with the mother phase by drop–interface coalescence.

3.2. Models of the Coalescence of Drop Swarms at Horizontal Plain Interfaces

3.2.1. *Survey on the Models*

Table 2 is a collection of published models on the coalescence of drop swarms at horizontal interfaces in primary dispersions. Many of these models are of an empirical nature, as mentioned in the Introduction. The experiments were carried out with mixer-settlers (horizontal settlers) or in spray columns (vertical settlers) by using different liquid systems depending on the point of view of the various authors. The corresponding classification can be drawn from Table 2. Apart from the empirical models, some authors have provided formulation for theoretical descriptions.

Most authors focus on the continuous settling process, but some try to work out a relationship between a batch experiment and a corresponding continuously operated settler. However, not all authors are of the opinion that these serve their purpose. Vieler, Glasser, and Bryson (*34*) or Godfrey, Chang-Kakoti, and Slater (*35*) detected no relationship between batch and continuous settlers although they carried out a multitude of experiments. They presume that, among other reasons, the different fluid-dynamic processes occurring during settling are responsible for the inability to transfer batch results to continuous settlers. The reason is that the settling process in a batch settler occurs under almost ideal conditions, e.g., sedimentation and coalescence take place in a calm, undisturbed flow regime while an additional motion from outside is forced upon continuous operated settlers. Over the past few years, Hartland and Jeelani (*36–40*) have reported that the required transfer is possible within the framework of well-defined and sharply restricted boundary conditions. Very important preconditions are the equality of drop sizes or drop size distributions, and of the flow conditions in both the batch experiment and the continuously operated settler.

3.2.2. *Batch Settling Process*

Discontinuous phase separation happens exclusively in dense dispersion bands of equal thickness over the entire settling surface. Batch experiments have been carried out in discontinuously operated mixers (*32*, *33*, *35–51*,

53–57, 78) and in stand jars (*58, 59*), with the exception of the experiments by Hartland (*8, 60, 61*) who used a spray column.

The height of the dense dispersion layer in the beginning of a batch settling experiment generally depends on the mixing power which is supplied to the two-phase system and which defines the drop size distribution. Additionally, in the case of stirring and shaking, the mixing duration (and in the case of jet break at orifices, the hole diameter and number) is of great influence. The phase ratio, which can be chosen freely only for the first two types of mixing, the liquid contents, and the type of dispersion influence the height of dispersion considerably, too.

All the authors cited started with ideal dispersions of uniform initial drop size distribution. The investigations aimed for the static settling time of a primary dispersion. In most cases it has to be determined experimentally as shown in Table 2. Reissinger et al. (*59*) reported that the static settling time can be roughly estimated from the density difference according to Figure 7, while all other material properties and parameters such as the drop size were neglected. But deviations from the corresponding measured values are considerably high. Slater and Ritcey (*47*) obtained an equation which allows computation of the static settling time from geometric and hydrodynamic parameters. The formulation of Loebmann and Blass (*57*) requires additional parameters which characterize the mixing process, e.g., the resulting drop size and material properties.

Figures 8 and 9 illustrate the typical shapes of measured settling curves, but only the models in References *37, 51, 55, 56,* and *78* can reproduce the more or less marked sigmoidal shape of the curve. In addition, cor-

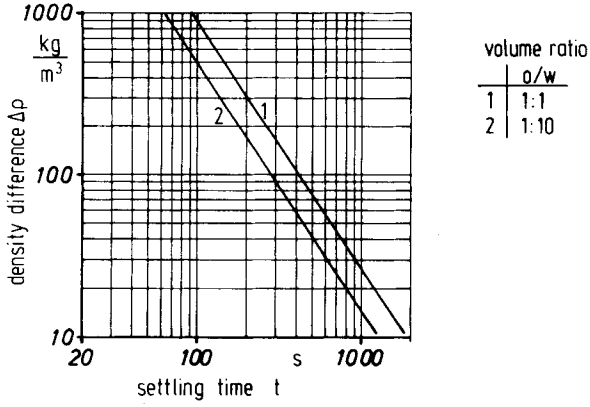

FIG. 7. Dynamic settling times for aqueous–organic systems according to Gillespie and Rideal (*20*).

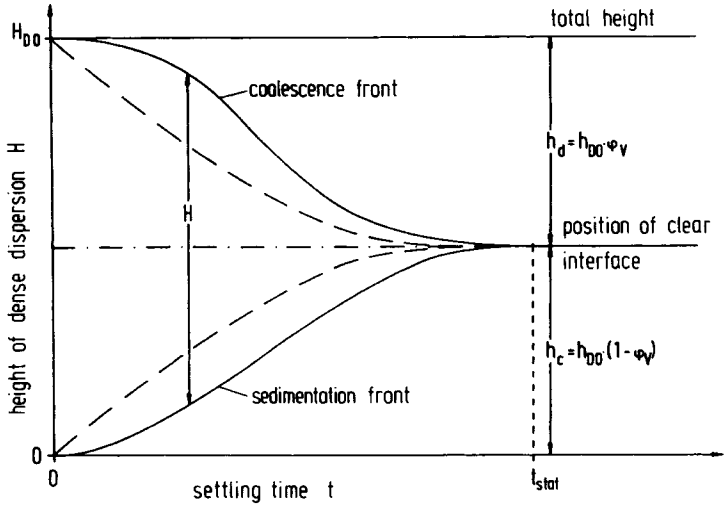

FIG. 8. Typical shape of a measured settling curve.

relation computations are necessary because between two and four constants have to be determined simultaneously. The computation results can only be proved by the experiment itself, because the calculated course of the curve is highly dependent on the initial values. It should be mentioned that sigmoidal settling curves not only arise in the case of the gravity settling

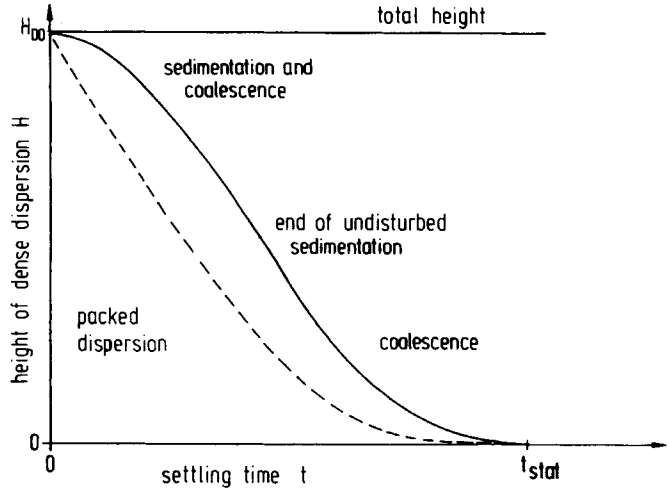

FIG. 9. Alteration in time of the height of the dense dispersion of a decreasing dispersion.

of primary dispersions but also in the case of the batch separation of secondary dispersions with the aid of thermal and electrical energy, ultrasonic, centrifugal energy (*62*), or solid additives like powder or granulate (*63*).

Since the duration of the settling process is strongly determined by the mean drop diameter at the beginning of settling (*29*, *47*, *51*, *57*, *64*, *65*), the course of the settling curve is no measure for the settling behavior in a continuously operated settler. Figure 10 illustrates the relationship between the mean initial drop size and the static settling time in dimensionless form, whereby the settling time is substituted for by the static settling velocity (*66*). The abscissa shows the dimensionless settling time.

$$(\mathrm{Re\ Fr})^{1/3} = v_{d,stat} \frac{\rho_c}{g\eta_c} \frac{\rho_c}{|\Delta\rho|} \tag{1}$$

with

$$v_{d,stat} = \frac{H_0 \varphi_V}{t_{stat}} \tag{2}$$

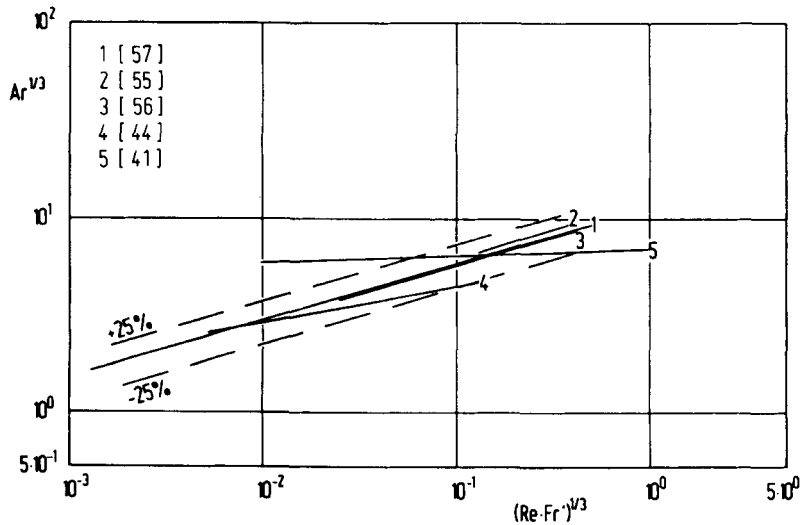

FIG. 10. Dependence between static settling velocity and initial mean drop size according to Reference 66.

and the ordinate the dimensionless mean drop diameter

$$Ar^{1/3} = d_{32}^2 \frac{\rho_c^2 g}{\eta_c^2} \frac{|\Delta\rho|}{\rho_c} \tag{3}$$

In their latest paper, Hartland and coworkers (*36*) distinguish between settling curves of sigmoidal and exponential shape without inflection points. They report that no formation of a coalescence zone takes place if the rate of sedimentation is lower than the rate of drop–interface coalescence throughout the whole settling process. In this case the settling curve exhibits an exponential shape (see Fig. 11b) and the coalescence process at the interface is only governed by the height of the dispersion band; while any relationship to the drop size can be neglected. The sigmoidal shape of the settling curve points to a coalescence mechanism which depends strongly on the drop size, while the height of the dense dispersion is of almost no importance (see Fig. 11a).

The previous section showed that batch experiments are very useful for obtaining qualitative information on the problems connected to the special liquid system, e.g., on the qualitative influence of mixing intensity, phase ratio, temperature, and surfactants. However, results drawn from batch experiments can only be transferred to continuously operated settlers if the boundary conditions, namely the identity of drop size distribution, flow conditions, and material properties, are strictly obeyed. In the case of a settler design, these requirements can hardly be fulfilled.

3.2.3. Continuous Settling Process

The genealogical tree of settler models in Fig. 12 shows that, in principle, stochastic and deterministic models can be distinguished. Hosozawa et al.

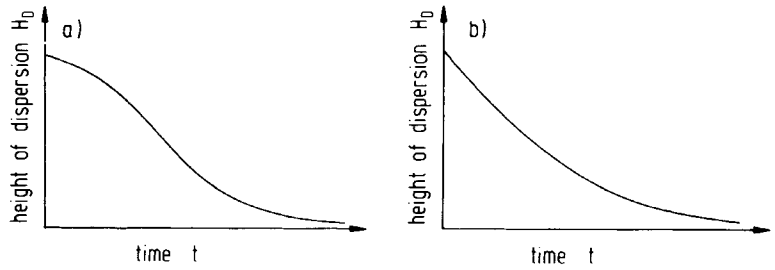

FIG. 11. Typical shapes of settling curves when the coalescence process is governed by the drop size (a) and when it is governed by the interfacial coalescence rate (b) according to Hartland et al. (*36*).

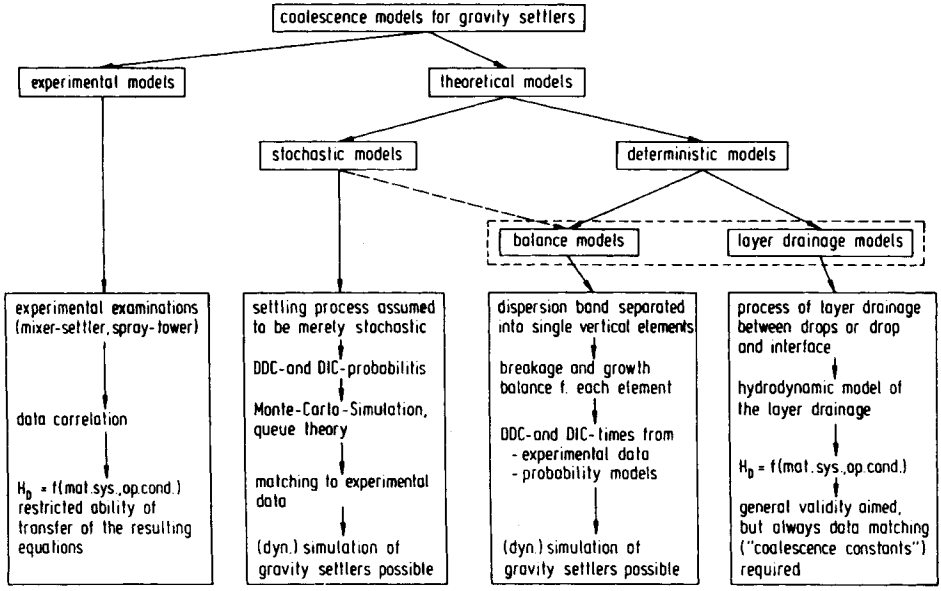

FIG. 12. Genealogical tree of continuously operated settlers models.

(*64*) and Doulah and Davies (*7*) assume the coalescence of drop swarms at a horizontal interface to be a stochastic process. They simulate it on the computer by means of the Monte-Carlo or the waiting queue method by using special probability functions for the drop–drop and drop–interface coalescence. The simulation models are adapted to their special boundary conditions by fitting the probability functions to experimental data. The authors could not obtain any possibility of a prediction of those probabilities, so the models cannot be transferred to other boundary conditions and are not suitable for a settler design. Therefore, no further details of these models are discussed in this paper.

Reissinger et al. (*59*) and Slater and Ritcey (*47*) apply the conclusions from the batch settling time directly to the continuous settling process. The models of Barnea and Mizrahi (*32*, *33*, *45*, *46*) and Golob and Modic (*49*) allow the same conclusion if the batch experiments were carried out by using a standard stand glass and applying equal hold-ups in the batch experiment and the feed of the continuously operated settler. The dynamic settling time is computed from the static one by using various empirically fitted parameters. All other authors who have dealt with a relation between batch and continuous settlers need additional information on the shape of the settling curve. As mentioned in Section 3.2.2, Hartland and coworkers

(*36–40*) developed a model to transfer the results drawn from batch experiments to the continuous process if the batch experiment is carried out with identical drop size distribution, material properties, and flow conditions. The model is based on layer drainage, and its empirical constants can be drawn from the batch settling curve.

The application of the models depends on whether the drop swarm coalescence takes place in a vertical or a horizontal settler. In a vertical settler the dispersed and continuous phase flow countercurrently through the apparatus. Most of the authors conducted their experiments with a static continuous phase. In the case of mixer–settler devices, one has to distinguish additionally whether it is a one- or a multistage apparatus. In a multistage device, both phases flow countercurrently through the whole device, while a one-stage device exhibits cross-countercurrent. Figures 13 and 14 provide schematic illustrations of these types.

Blass, Loebmann, Meon, and Rommel (*66*) compared some of the reviewed models with the help of a specially developed computer program. They found that only a few models can correctly be applied to other (testing) conditions in addition to the original ones of each model. Those models which could be compared showed identical tendencies in their results. The height of the dense dispersion increases with growing drop diameters and

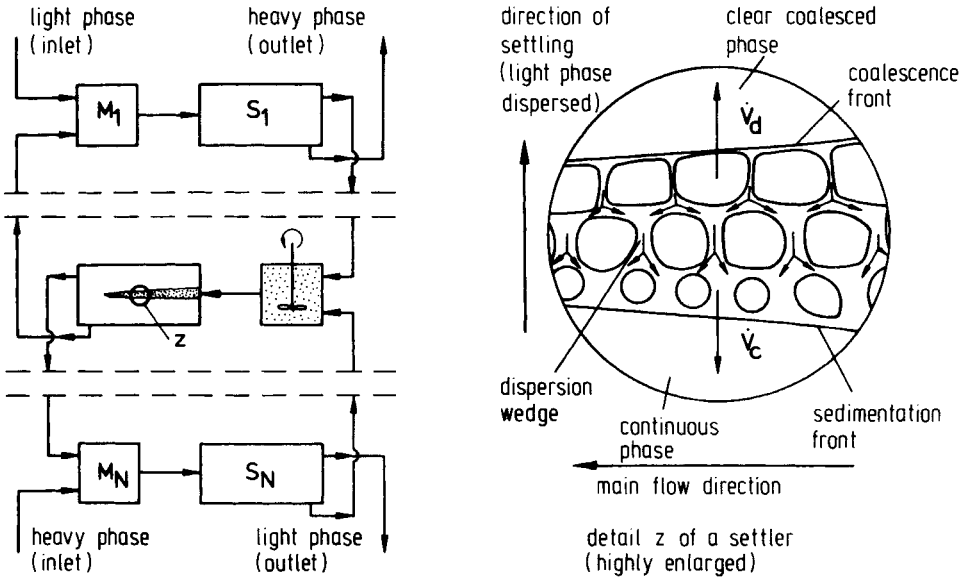

FIG. 13. Schematic illustration of phase flow in a vertical settler.

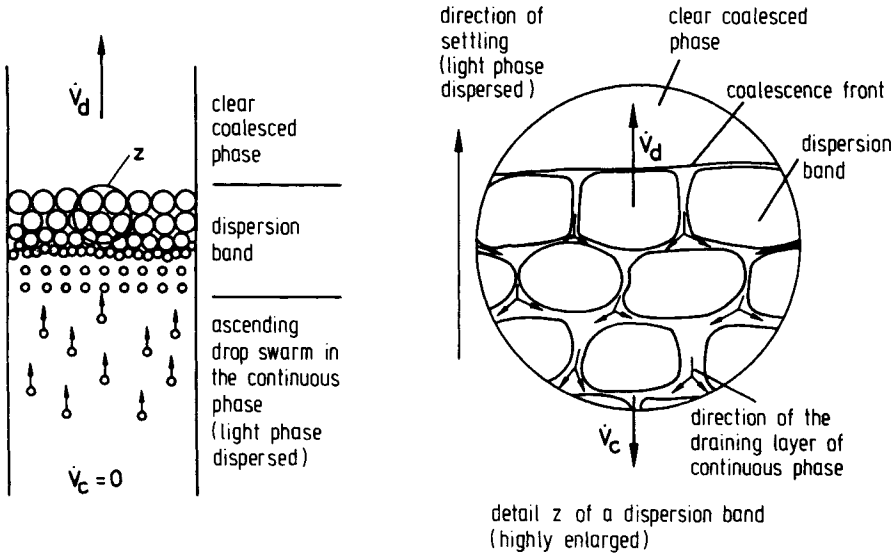

FIG. 14. Schematic illustration of phase flow in a horizontal settler.

with increasing loads of the dispersed phase. The calculated absolute values of the steady-state height differ considerably. The experimental results conducted by some authors are well reproducible by their own equations in many cases, but even some of the models sometimes fail in these cases. The reason is that besides the common material properties and the operation conditions, additional effects and boundary conditions have a strong influence on the coalescence process. That means that the models can only work within the frame of the conditions on which the deduction of the model is based. So far, attempts to transfer them to other boundary conditions have not been successful.

4. SUMMARY

The coalescence process, i.e., the flowing together of two drops or of a drop and a coherent liquid layer, is governed by the drainage and rupture of a thin liquid layer which separates the two coalescence partners. The drainage process is affected by a multitude of parameters. Although many of those effects and their influence on coalescence is well known in a phenomenological way, no practically applicable models exist which describe the influence of surfactants, of intermolecular interactions, of electric effects, and of the influence of mass transfer. All models are based purely on hydrodynamic considerations.

Only recently have the models for single drop coalescence begun to regard intermolecular interactions on the drainage process by applying the Hamaker coefficient. However, the sensitivity of this coefficient on the computation results is not very large. Modeling of the coalescence of drop swarms in dense dispersions has been done with both stochastic and deterministic models. Stochastic models always require experiments on a real, continuously operated settler in order to evaluate the probability parameters. They allow simulation of existing settlers but they are not applicable for settler design. Deterministic models which require no experiments lead to insufficient results because they cannot evaluate nonhydrodynamic effects on the coalescence process. Those deterministic models which require additional experiments allow settler design in principle. Depending on the model, the experiments are carried out with batch or continuous settlers in which all boundary conditions have to be obeyed, but the models need information on the drop size and/or the hold-up profile and/or the turbulent conditions in the dispersion zone. Normally, this information is not available in the settler design step.

Finally, a settler design based only on hydrodynamics cannot lead to satisfactory results. Additional effects, described above, must be incorporated.

NOTATION

A	cross-sectional area of the settler (m^2)
C, C_f, C_c	fitting parameters (—)
C_1, C_2	constants (—)
D_{iS}	diameter of settler inlet tube (m)
D_W	height of the inlet weir (m)
d_p	drop diameter (m)
f_0	characteristic function (—)
g	gravity acceleration (m/s^2)
$H_{c,d}$	Hamaker coefficient (J)
$\hat{H}_{c,d}$	London–Hamaker coefficient = 1.13×10^{-28} J·m
H_D	height of the dense dispersion in a continuous settler (m)
h_D	height of the dense dispersion in a settler (m)
$h_{D,0}$	initial height of the dense dispersion (m)
K	constant (—)
L	height of the drop above the interface (m)
L_D	length of the dispersion wedge (m)
$L_{D,iS}$	length of the dispersion wedge at the settler inlet (m)
n_M	number of revolutions per minute (min^{-1})
r	radial distance, related radius (m)
r_f	radius of the contact area (m)

R	radius of curvature of the contact area (m)
T	mean residence time in the settler (s)
t	time (s)
t_k	time of coalescence (s)
t_{stat}	static settling time (s)
$\dot{V}$	volumetric flow rate (m^3/s)
$\dot{V}_c$	volumetric flow rate of the continuous phase (m^3/s)
$\dot{V}_d$	volumetric flow rate of the dispersed phase (m^3/s)
$\dot{V}_{d,Flut}$	volumetric flow rate of the dispersed phase at flooding conditions (m^3/s)
$\dot{V}_{grenz}$	limiting load of a settler (m^3/s)
v	velocity (m/s)
v_c	superficial velocity of the continuous phase (m/s)
v_d	superficial velocity of the dispersed phase (m/s)
$v_{c,stat}$	static settling velocity of the continuous phase (m/s)
$v_{d,stat}$	static settling velocity of the dispersed phase (m/s)
v_{iS}	superficial velocity profile at the settler inlet (m/s)
w_{rS}	relative swarm velocity (m/s)
y	exponent (—)
γ_i	shape factor (—)
δ	thickness of the layer (m)
$\delta(t)$	time depending value of the thickness (m)
δ_c	critical thickness (m)
η_c	dynamic viscosity of the continuous phase (kg/ms)
η_d	dynamic viscosity of the dispersed phase (kg/ms)
θ	angle (degrees)
θ_D	mean residence time in the dense dispersion (s)
φ_V	phase ratio (—)
ρ_c	density of the continuous phase (kg/m^3)
ρ_d	density of the dispersed phase (kg/m^3)
σ	interfacial tension (N/m)
τ_D	mean time of binary coalescence (s)
τ_{DI}	mean time of interfacial coalescence (s)

REFERENCES

1. M. Bohnet, *Chem.-Ing.-Tech.*, *48*(3), 177–189 (1976).
2. E. Blass and D. Rautenberg, *German Chem. Eng.*, *7*(3), 207–211 (1984).
3. S. Hartland, *Trans. Inst. Chem. Eng.*, *45*, 97–114 (1967).
4. T. D. Hodgson and D. R. Woods, *J. Colloid Interface Sci.*, *30*(4), 429–446 (1969).
5. D. T. Wasan and A. K. Malhotra, *AIChE Symp. Ser.*, *82*(252), 5–13 (1986).
6. J. D. Chen, P. S. Hahn, and J. L. Slattery, *AIChE J.*, *34*(1), 140–143 (1988).
7. M. S. Doulah and G. A. Davies, *Proc. ISEC'74, Lyon, 1974*, pp. 533–549.
8. S. Hartland and D. K. Vohra, *J. Colloid Interface Sci.*, *66*(1), 1–11 (1978).

9. M. Perrut and R. Loutaty, *Gen. Chim., 103*(19), 2545–2556 (1970).
10. G. V. Jeffreys and G. A. Davies, "Coalescence of Liquid Droplets and Liquid Dispersions," in *Recent Advances in Liquid–Liquid Extraction* (C. Hanson, ed.), Pergamon, 1971.
11. D. R. Woods and K. A. Burril, *J. Electroanal. Chem., 37,* 191–213 (1972).
12. H.-D. Pabst, Doctoral Thesis, University of Dortmund, FRG, 1975.
13. A. D. Hovarongkura, Thesis, West Virginia University, USA, 1979.
14. B. Drogaris, Doctoral Thesis, University of Dortmund, FRG, 1983.
15. G. V. Jeffreys and T. L. Hawksley, *AIChE J., 11*(3), 413–424 (1965).
16. G. V. Jeffreys and G. B. Lawson, *Trans. Inst. Chem. Eng., 43,* 294–298 (1965).
17. G. A. Davies, G. V. Jeffreys, and D. V. Smith, *Proc. ISEC'71, The Hague,* 1971, Paper 35.
18. G. E. Charles and S. G. Mason, *J. Colloid Sci., 15,* 105–122, 236–267 (1960).
19. G. B. Lawson, Thesis, University of Manchester (UMIST), UK, 1967.
20. T. Gillespie and E. K. Rideal, *Trans. Faraday Soc., 52,* 73–183 (1956).
21. S. B. Lang and C. R. Wilke, *Ind. Eng. Chem., Fundam., 10*(3), 329–352 (1971).
22. S. P. Frankel and K. J. Mysels, *J. Phys. Chem., 66*(1–5), 190 (1960).
23. J. D. Chen, P. S. Hahn, and J. C. Slattery, *AIChE J., 30*(4), 622–630 (1984).
24. H. M. Princen, *J. Colloid Sci., 18,* 178–195 (1963).
25. H. M. Princen, *Ibid., 24,* 1–84 (1969).
26. Y. A. Buevich and E. K. Lipkina, *Colloid J. USSR, 40*(2), 201–206 (1978).
27. A. Vrij and J. T. G. Overbeek, *J. Am. Chem. Soc., 90,* 3074–3078 (1968).
28. J. D. Robinson and S. Hartland, *Proc. ISEC'71, The Hague, 1971,* pp. 418–427.
29. A. Hitit, Thesis, University of Aston, Birmingham, UK, 1972.
30. A. M. A. Allak and G. V. Jeffreys, *AIChE J., 29*(3), 564–569 (1974).
31. A. M. A. Allak and G. V. Jeffreys, *Proc. ISEC'74, Lyon, 1974,* pp. 265–288.
32. E. Barnea and J. Mizrahi, *Trans. Inst. Chem. Eng., 53,* 61–69 (1975).
33. E. Barnea and J. Mizrahi, *Ibid., 53,* 70–74 (1975).
34. A. M. S. Vieler, D. Glasser and A. W. Bryson, *Proc. ISEC'77, Toronto, 1977,* pp. 399–406.
35. J. C. Godfrey, D. K. Chang-Kakoti, and M. J. Slater, *Ibid.,* pp. 406–412.
36. S. Hartland and S. A. K. Jeelani, *Chem. Eng. Sci., 42*(8), 1927–1938 (1987).
37. S. A. K. Jeelani and S. Hartland, *AIChE J., 31*(5), 711–720 (1985).
38. S. A. K. Jeelani, Doctoral Thesis, ETH Zurich, Switzerland, 1986.
39. S. A. K. Jeelani and S. Hartland, *Chem. Eng. Prog., 20,* 271–276 (1986).
40. S. A. K. Jeelani and S. Hartland, *Chem. Eng. Res. Des., 64*(6), 450–460 (1986).
41. W. A. Rodger, Argonne National Laboratory, ANL-5575, Argonne, Illinois, USA, 1956.
42. A. D. Ryon, F. L. Daley, and R. S. Lowrie, Oak Ridge National Laboratory, ORNL-2951, Oak Ridge, Tennessee, USA, 1960.
43. A. D. Ryon, F. L. Daley, and R. S. Lowrie, Oak Ridge National Laboratory, ORNL-3381, Oak Ridge, Tennessee, USA, 1963.
44. G. Lewis, Thesis, University of Wales, Swansea, UK, 1966.
45. E. Barnea and J. Mizrahi, *Trans. Inst. Chem. Eng., 53,* 75–82 (1975).
46. E. Barnea and J. Mizrahi, *Ibid., 53,* 83–92 (1975).
47. M. J. Slater, G. D. Ritcey, and R. F. Pilgrim, *Proc. ISEC'74, Lyon, 1974,* pp. 107–140.
48. D. C. Lindholm and R. G. Bautista, *Trans. Am. Inst. Mech. Eng., 260*(3), 1–5 (1976).
49. J. Golob and R. Modic, *Trans. Inst. Chem. Eng., 55,* 207–211 (1977).
50. P. D. Middlebrook, Thesis, University of Bradford, UK, 1980.
51. D. G. Austin and G. V. Jeffreys, *J. Chem. Technol. Biotechnol., 31,* 475–488 (1981).
52. H. M. Stoenner and F. Woehler, *J. S. Afr. Inst. Min. Metall., 82*(4), 97–105 (1982).

53. H.-J. Weiss, *Chem. Technol. (Leipzig), 34*(6), 308–311 (1982).
54. B. Moyer and W. J. McDowell, *Sep. Sci. Technol., 18*(14/15), 1535–1562 (1983).
55. N. Siemons, *IVT—Inf. RWTH Aachen, 13*(2), 22–29 (1983).
56. N. Siemons, Doctoral Thesis, RWTH Aachen, FRG, 1985.
57. A. Loebmann and E. Blass, Actes du Colloque "Extraction par Solvent et Echange d'Ion," Toulouse, 1985, France, Paper IIIB.
58. R. C. Lock, *Q. J. Mech. Appl. Math., 4,* 42 (1951).
59. K. H. Reissinger, J. Schroeter, and W. Baecker, *Chem.-Ing.-Tech., 53*(8), 607–614 (1981).
60. S. Hartland, *Ber. Bunsenges. Phys. Chem., 85,* 851–863 (1981).
61. S. Hartland, *Tenside Deterg., 18*(4), 178–189 (1981).
62. E. A. Lack, Thesis, Technical University of Graz, Austria, 1981.
63. J. Mizrahi and E. Barnea, *Br. Chem. Eng., 15*(4), 497–503 (1970).
64. M. Hosozawa, M. Suzuki, T. Tadaki, and S. Maeda, DRIC Translation No. 3507, 1973.
65. K. T. Hossain, S. Sarkow, C. Y. Mumford, and C. R. Phillips, *Ind. Eng. Chem., Process Des. Dev., 22,* 553–563 (1983).
66. E. Blass, A. Loebmann, W. Meon, and W. Rommel, *Chem.-Ing.-Tech., 61*(8), 597–610 (1989).
67. A. D. Ryon, F. L. Daley, and R. S. Lowrie, *Chem. Eng. Prog., 55*(10), 71–75 (1959).
68. S. Gondo and K. Kusunoki, *Hydrocarbon Process., 9,* 209–210 (1969).
69. G. A. Davies, G. V. Jeffreys, D V. Smith, and F. A. Ali, *Can. J. Chem. Eng., 48,* 328–329 (1970).
70. D. V. Smith and G. A. Davies, *Ibid., 48,* 628–637 (1970).
71. A. M. A. Allak, PhD Thesis, Aston University, Birmingham, UK, 1973.
72. H.-D. Pabst, Doctoral Thesis, University of Dortmund, FRG, 1975.
73. H. M. Stoenner and F. Woehler, *Ind. Chem. Eng. Symp. Ser., 42,* 1–13 (1975).
74. S. Vijayan and A. B. Ponter, *Tenside Deterg., 13*(4), 193–200 (1976).
75. D. C. Drown and W. Y. Thomson, *Ind. Eng. Chem., Process Des. Dev., 16,* 197–206 (1977).
76. A. N. Kumar, D. K. Vohra, and S. Hartland, *Can. J. Chem. Eng., 58,* 154–159 (1980).
77. F. M. Gomez and H. Wilkinson, *Proc. ISEC'80, Lyon, 1980,* Paper 20–37.
78. H. M. Stoenner and P. Wiesner, *J. S. Afr. Inst. Min. Metall., 82*(4), 97–195 (1982).
79. T. Misek, *Proc. ISEC'86, Munich,* 1986, pp. III-71–III-79.
80. H. H. Shen and Z. J. Shen, *Ibid.,* pp. III-431–III-436.
81. C. Gourdon, G. Muratet, and C. Casamatta, *Ibid.,* pp. III-361–III-368.
82. Y. M. Jiang, B. Y. Sun, and Q. Zhao, *Ibid.,* pp. III-225–III-230.
83. W. Dalingaros and S. Hartland, *Can. J. Chem. Eng., 64*(6), 925–930 (1986).
84. S. A. K. Jeelani and S. Hartland, *Proc. ISEC'88, Moscow, 1988,* pp. II-128–II-131.
85. L. I. Sklokin, V. E. Leif, and S. M. Masloboyeva, VINITI 12.12.78, N 3786.
86. L. I. Sklokin, V. E. Leif, and S. M. Masloboyeva, *Proc. ISEC'88, Moscow, 1988,* pp. II-132–II-135.

Received by editor January 22, 1991